Nuclear Inst. and Methods in Physics Research, A 975 (2020) 164197

Contents lists available at ScienceDirect

Nuclear Inst. and Methods in Physics Research, A

journal homepage: www.elsevier.com/locate/nima

Tl concentration and its variation in a CsI(Tl) crystal for the CALIFA detector

A. Knyazev [a], J. Park [a,j], P. Golubev [a], J. Pallon [a], J. Cederkall [a,*], H. Alvarez-Pol [b], J. Benlliure [b], J.A. Briz [c], P. Cabanelas [b], E. Casarejos [d], D. Cortina-Gil [b], P. Díaz Fernández [e], M. Feijoo [b], D. Galaviz [f], E. Galiana [f], M.J.G. Borge [c], R. Gernhäuser [g], D. Gonzalez [b], C. Gutierrez-Neira [h], A.-L. Hartig [i], A. Heinz [e], B. Heiss [g], H. Johansson [e], P. Klenze [g], T. Kröll [i], T. Nilsson [e], A. Perea [c], L. Ponnath [g], H.-B. Rhee [i], J.L. Rodriguez-Sanchez [b], O. Tengblad [c], P. Teubig [f]

[a] Department of Physics, Lund University, SE-221 00 Lund, Sweden
[b] Dpt. de Física de Partículas, Universidade de Santiago de Compostela, E-15782 Santiago de Compostela, Spain
[c] Instituto de Estructura de la Materia, CSIC, E-28006 Madrid, Spain
[d] Universidade de Vigo, E-36310 Vigo, Spain
[e] Department of Physics, Chalmers University of Technology, S-41296 Gothenburg, Sweden
[f] Laboratory for Instrumentation and Experimental Particle Physics, 1649-003 Lisbon, Portugal
[g] Physik Department, Technische Universität München, 85748 Garching, Germany
[h] Centro de Micro-Analisis de Materiales, Universidad Autonoma de Madrid, E-28049, Madrid, Spain
[i] Institut für Kernphysik, Technische Universität Darmstadt, D-64289 Darmstadt, Germany
[j] Center for Exotic Nuclear Studies, Institute for Basic Science (IBS), 34126 Daejeon, Korea

ARTICLE INFO

Keywords:
Nuclear reactions
Calorimeters
Scintillators
CsI(Tl) energy resolution

ABSTRACT

One of the factors that can contribute to the resolution of long, doped inorganic scintillators used for nuclear spectroscopy is the variation of the dopant concentration over the length the detector crystal. In this work an investigation of such potential variations in one of the CsI(Tl) scintillators used in the calorimeter, CALIFA, of the R^{3}B experiment at FAIR, has been performed using particle induced X-ray emission. No statistically significant gradient in doping level was found along the long axis of the investigated sample crystal and the mean value of the Tl concentration was measured to be 0.0839(38)% by weight. This corresponds to a light output of $97.3^{+1.3}_{-1.7}$% relative to the maximum attainable light output according to previously published work. By taking the $\pm 1\sigma$ bounds, the 3% statistical spread in the relative light output provides a good reference value of the minimum light-output non-uniformity observed for the CALIFA crystals. If the relative light output is estimated pointwise from a set of Tl concentration measurements a light-output non-uniformity of 4.6(2.4)% results. For a γ-ray energy of 662 keV the deduced variation in Tl concentration contributes with 0.48(6)% to the typical resolution of 7.74(6)% measured with a collimated source along the crystal main axis. The result is of interest for the characterization of the detector system performance and for realistic simulations of the light collection process in detector systems that are used for nuclear spectroscopy and calorimetry.

1. Introduction

1.1. Purpose of the study

In order to properly characterize the performance of a multidetector system that uses scintillation as detection mechanism for spectroscopic measurements, several different effects need to be considered. Specifically, for a case where long frustum-shaped detector elements are used, light collection from different parts of the detector volume will be influenced both by absorption of the scintillation light, and by its reflection at the boundaries of the detector volume [1,2]. This problem becomes particularly interesting for a case where high-energy γ-rays and charged particles from a nuclear reaction are to be detected using the same detector system since measurement of the energy carried by one photon or charged particle often requires summing of signals from several detector elements. If significant non-uniformity in light output exists between the different parts of the detector volume it will translate into a loss of overall resolution.

We, as well as other authors, have addressed light absorption and reflective properties for detectors built on scintillator elements in previous work [1–4] and also discussed how one can minimize its influence on the detector response. However, one effect where more detailed information would be beneficial, e.g. for detector simulations, is the

* Corresponding author.
E-mail address: joakim.cederkall@nuclear.lu.se (J. Cederkall).

https://doi.org/10.1016/j.nima.2020.164197
Received 21 February 2020; Received in revised form 25 May 2020; Accepted 27 May 2020
Available online 29 May 2020

influence of doping concentration variations on light output and its variation, and on resolution.

In this work we address this issue by performing a PIXE measurement on a CsI(Tl) crystal of the CALIFA calorimeter of the R^{3}B experiment at FAIR. In the following we give a short physics motivation for the construction of the R^{3}B experiment and the design chosen for the elements of the CALIFA calorimeter. We then discuss the effects this design has on scintillation light collection. This is followed by a description of the procedure used for the PIXE measurement, and a discussion of the analysis of the data and the conclusions that can be drawn from the measurement.

1.2. General detector considerations for experiments with high-energy radioactive beams

The investigation of exotic nuclear systems far from stability using radioactive ion beams is a key topic in current experimental nuclear physics. Several new facilities exist or are under construction worldwide for experiments in this field [5–11]. The drive towards the most exotic nuclear systems typically takes place at fragmentation facilities, where a heavy-ion beam at relativistic velocity is fragmented by a light target and the in-flight separated products are let to impinge on a secondary target where the nuclear reaction of interest takes place. This technique does not only facilitate the production of very short-lived atomic nuclei but also makes it possible to transport the exotic beam in very short time to the experimental stations and therefore minimizes decay loss before the exotic isotope under study reaches the detector system.

Radioactive beams produced in this manner can be of quite low intensity. However, the high energy of the beams produced with this technique provides advantages, e.g. better utilization of the beam, as a thick secondary reaction target can be used. The high energy also leads to a set of specific requirements for calorimeter-like detectors that surround the secondary target position. One requirement for such a setup is the ability to detect the reaction products and to perform γ-ray spectroscopy simultaneously. A solution to this challenge is to use a detector with high granularity and elongated detector modules that possess a high stopping power. The high granularity allows reconstruction of the energy of Lorentz-boosted γ-rays emitted in-flight, while the high-Z dense material is effective for stopping the reaction products and to increase the cross section for γ-ray detection.

2. Light collection in CALIFA detector modules

2.1. The CALIFA design in brief

The current work concerns the performance of detector elements of the CALorimeter for In-Flight detection of γ-rays and light charged pArticles (CALIFA) [12], of the Reactions with Relativistic Radioactive Beams (R^{3}B) [13] experiment at the Facility for Antiproton and Ion Research (FAIR) [5]. CsI(Tl) was chosen as the dominant sensitive material for the calorimeter as it is only weakly hygroscopic [14] and has good stopping power and scintillation properties. Applying the requirements mentioned above to R^{3}B [15] results in a calorimeter design with thin elongated frustum shapes of the detector elements and crystal lengths from 17 up to 22 cm. The good hygroscopic properties of CsI(Tl) also reduce the amount of casing material otherwise needed in the setup, and thus lead to higher detector efficiency as well as better efficacy for the energy add-back procedures [2] employed in high-granularity γ-ray spectrometers. In CALIFA each CsI(Tl) detector crystal is coupled to an APD for scintillation light readout. Amplification and data collection is performed via a custom-designed readout chain. For more information about the detector design see e.g. Refs. [15–18].

2.2. Contributions to the resolution

One of the most important characteristics of a spectrometer is its energy resolution. The resolution is often separated into three terms [19,20]:

$$(\Delta E/E)^2 = \delta_{\mathrm{sc}}^2 + \delta_{\mathrm{st}}^2 + \delta_{\mathrm{tr}}^2, \tag{1}$$

where δ_{sc} is the intrinsic resolution of a crystal material, δ_{st} is the contribution from the statistical variation in the number of electrons produced in the light sensor, and δ_{tr} is the variation in light collection that arises from the light transport in the scintillator. We have investigated contributions to δ_{tr}^2 and δ_{st}^2 for the CALIFA detector elements in a previous work [2], with a focus on variations in light collection from different parts of the detector volume caused by the detector geometry, and variations in gain of the APD as a function of temperature. As discussed in that work the interplay of light absorption and focussing, caused by the tapered shape of the crystals, gives rise to a position dependent light-output curve for a polished crystal where more scintillation photons are detected from scintillation events that occur further away from the APD. This effect, known as the focussing effect, can to some extent be reduced in order to improve the overall energy resolution of the crystal. A common solution is either to lap the crystal surface or to modify the reflector. Similar studies, as presented for the current project in Ref. [2], where an Enhanced Specular Reflector (ESR) is used, are also discussed in Refs. [1,3,4,21], including the use of Teflon tape as reflector [1].

The δ_{sc} term relates to the level of doping for an inorganic scintillator. Doping introduces additional de-excitation centers in the crystal lattice which modifies the light emission spectrum and the decay constant of the scintillation flash. A detailed discussion of the effects of Tl doping of CsI can e.g. be found in Ref. [22]. Previous studies have established a relationship between Tl-doping concentration in CsI and the intensity of the scintillation flash [23,24]. Variations in doping concentration, and thus light output, over the crystal volume do not only influence the statistical spread, but also affect the number of photons collected from different parts of the detector volume, which in turn is reflected in the signal amplitude. Such variations would influence the resolution of the detector system in the same way as a position-dependent light collection caused by the focussing and absorption effects, with the difference that it cannot easily be improved by surface treatment.

3. Measurement procedure

3.1. Preparation of the sample crystal

The starting point for the Tl-concentration measurements was to prepare a 17 cm CALIFA sample crystal with minimized light-output non-uniformity, ΔLO, defined as:

$$\Delta\mathrm{LO} = \frac{C_{\max} - C_{\min}}{\frac{1}{N}\sum_{i=1}^{N} C_i} \times 100\%, \tag{2}$$

where $C_{\max}$ and $C_{\min}$ are the maximum and minimum centroid values of Gaussian fits of the photopeaks measured using a collimated γ-source in $N = 10$ equidistant points over the length of the crystal. In order to achieve this a polished crystal was lapped on the four lateral sides to reduce the effect of focussing and absorption. The sample crystal that was used for the Tl concentration measurements improved the light output non-uniformity from 13.45(6)% to 1.59(5)% after this procedure. The difference in performance before and after the surface treatment is presented in the left panel of Fig. 1.

The improvement in light output non-uniformity also enhanced the resolution from 13.26(4)% to 7.96(2)% at 662 keV for the same crystal. This resolution, which is discussed further in Section 4, is extracted for the sum peak measured at 662 keV using the collimated ^{137}Cs source in the 10 equidistant points along the main crystal axis. It should also

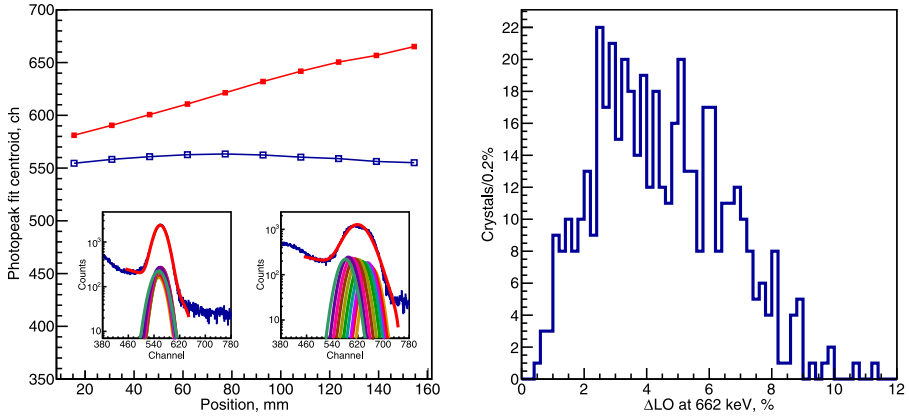

Fig. 1. Left panel: the light output of a 17 cm long frustum shaped CsI(Tl) crystal of the CALIFA project, measured with a 10 msr collimated ^{137}Cs γ-source, as given by the centroid of the photopeak. The red curve shows the result for a polished crystal, and the blue curve for the same crystal with lapping applied on the four lateral sides. The non-uniformity of the light output changes from 13.45(6)% to 1.59(5)% (see text for definition). The left and right insets show summed photopeaks from 10 equidistant points along the main axis of the crystal, measured with the collimated ^{137}Cs γ-source, together with fits of individual photopeaks for the lapped and polished surfaces, respectively. The distance is measured from the photosensor. See also Fig. 2 for the crystal geometry and Ref. [2] for further details on the measurement procedure and different effects that can influence the light-output non-uniformity. Right panel: Distribution of the light output non-uniformity measured, with a collimated γ-source at 662 keV, for a sample of 478 CALIFA CsI(Tl) detectors. The average light output non-uniformity of the set was found to be 4.47(9)%, which corresponded to an average resolution of 5.23(3)% at 1275 keV. One can notice a sharp drop in the distribution around $\sim$2−3%. For the definition of ΔLO see the text. (For interpretation of the references to color in this figure legend, the reader is referred to the web version of this article.)

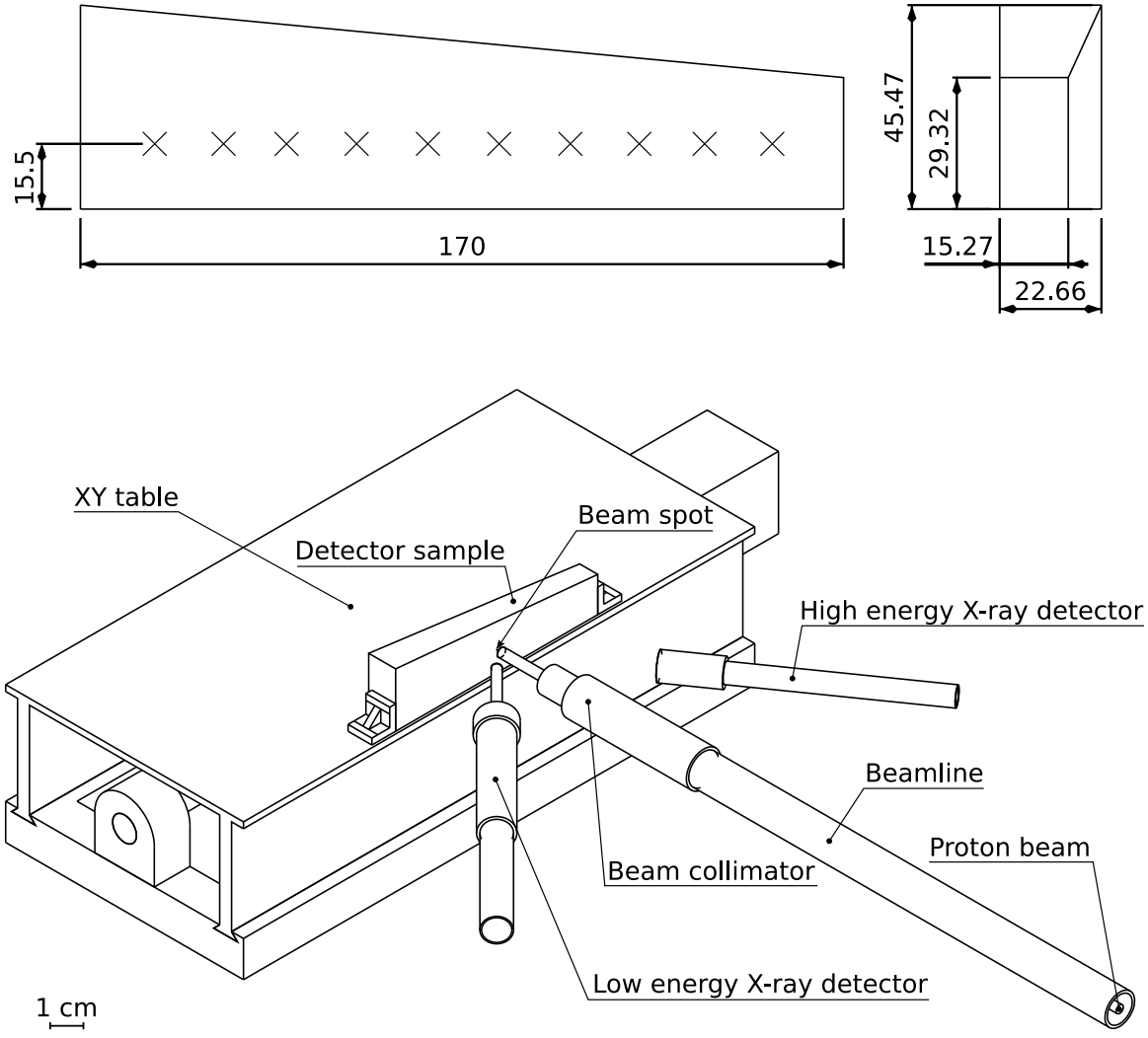

Fig. 2. A sketch of the sample crystal (top) and setup (bottom) used to measure the Tl concentration over the crystal length at CMAM. A high-energy X-ray detector was used to measure the Tl L- and Cs and I K-transitions and a low-energy X-ray detector was used to measure possible contaminants in the crystal. Ten equidistant points were measured on both sides of the sample crystal with additional measurements in three 5 × 5 mm^2 test areas at both ends and at the center of the crystal, respectively. This was done to investigate possible fluctuations of the Tl concentration over short distances. The positioning of the crystal was performed by an XYZ-table equipped with stepping motors.

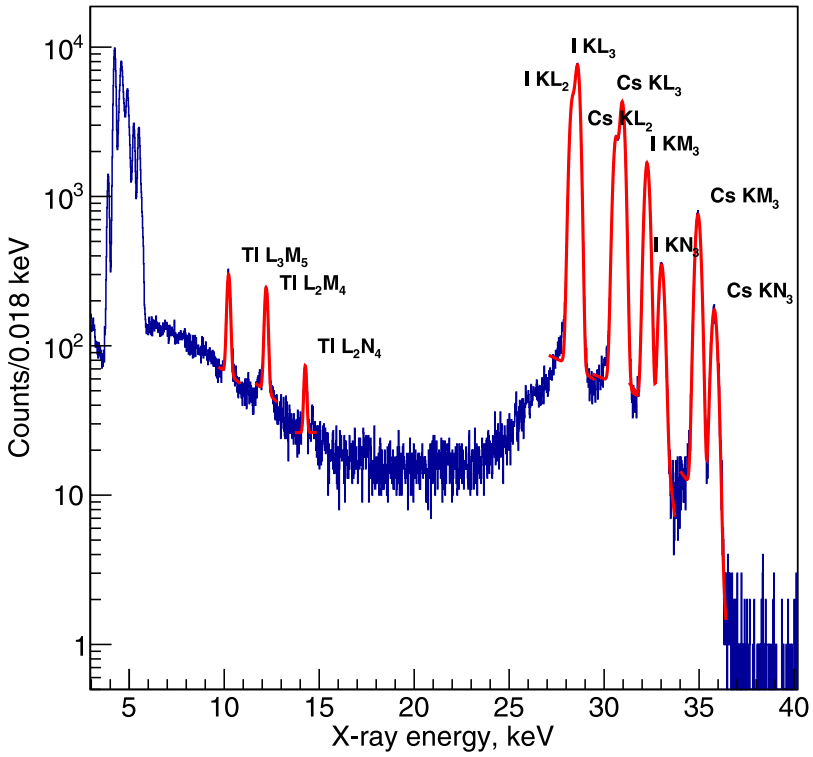

Fig. 3. An example of an X-ray energy spectrum measured at CMAM. The red lines show fits of the identified transitions, used for determination of the Tl concentration. The measured intensities were calibrated by using a reference crystal whose absolute concentration was measured at LIBAF. The low-energy part of the spectrum exhibits a combination of I L3-M5, L1-M2 lines, and Cs L2-N4, L1-N3 lines that were not used in the analysis. (For interpretation of the references to color in this figure legend, the reader is referred to the web version of this article.)

be mentioned that the resolution at 1275 keV improved from 12.0(5)% to 4.7(1)% when the crystal was irradiated with an uncollimated ^{22}Na source from the side. Further details of the measurements and the setup are given in Ref. [2].

The distribution of light output non-uniformity measured for a set of 478 crystals of the CALIFA geometry is shown in the right panel of Fig. 1. The prepared sample crystal falls into the group of crystals with comparatively small ΔLO $\lesssim 2-3\%$, where the residual non-uniformity of the light collection could be influenced by variations in dopant concentration over the crystal volume.

3.2. PIXE and Tl concentration

In order to quantify dopant-dependent variations in the intrinsic resolution, given by the δ_{sc}^2 term in Eq. (1), over the crystal length, it is necessary to find an independent way to determine the light output that does not rely on the same technique used to measure any effects caused by light focussing and absorption. For this reason we performed a measurement of the Tl concentration and its variation in the sample crystal using the Particle Induced X-ray Emission (PIXE) technique and related the Tl concentration to light output using previously published data [24].

A PIXE measurement of the Tl concentration in CsI(Tl) has been performed earlier and is reported in Ref. [25]. The objective in that work was to measure the dopant concentration in several different CsI(Tl) samples with the aim to compare the result to nominal values from the respective manufacturers, and to investigate the relative scintillation yield for α-particles and γ-rays as a function of Tl concentration. The aim in this work is on the other hand to measure the dopant concentration in different locations of the same crystal in order to determine to what extent variations in dopant concentration could influence the attainable resolution for a long frustum-shaped crystal. This provides an independent method to measure dopant-induced light-yield variations that otherwise are masked by the interplay of the focussing and absorption effects in tapered crystals.

The measurements were performed in two stages. Firstly, absolute values of the Tl concentration were determined for a reference crystal at the Lund Ion Beam Analysis Facility (LIBAF) in Lund, Sweden. Secondly, this reference crystal was also measured at the Centre for Micro Analysis of Materials (CMAM) of the Autonomous University of Madrid (UAM), Spain, and used to calibrate the measurement setup there. The CMAM setup was then used to measure the relative change in Tl concentration for the 17 cm long sample crystal whose light output non-linearity, before and after lapping, is given in Fig. 1. The details of these two measurements are given in the following.

3.3. Measurements at LIBAF

At LIBAF, a 2.57 MeV proton beam, with a diameter of 1 mm, was used. The characteristic X-rays from the reference crystal were detected with a 0.45 mm thick Si-drift detector with an area of 50 mm^2, covering a solid angle 40.8 msr. A 12.5 μm Be detector window, and a combined Be, Mylar and Al filter with a pinhole opening, were used to selectively suppress parts of the X-ray spectrum. The positioning of the sample, whose long axis was oriented in the direction perpendicular

to the beam, was provided by a set of stepping motors with precision of 10 μm. Since the measurement was performed in vacuum, it was necessary to coat the reference crystal with a thin carbon film to avoid discharges that otherwise can be caused by the charge transferred to the sample from the beam. The carbon coating does not influence the possibility to measure the Tl, Cs and iodine X-rays. The Tl concentration was measured, at 16.4 mm, and 163.6 mm from the end surface of the reference crystal, to be 0.0668(23) and 0.0667(18)% by weight, respectively. These data were used for absolute calibration of the data gathered at CMAM.

3.4. Measurements at CMAM

The CMAM measurements were performed using a three-axis ($X-Y-Z$) stepper motor stage in air using an extracted proton beam. The CMAM proton beam, with an energy of 3 MeV, was directed onto the sample at a distance of 4 mm from the beam port, providing a beam spot of 200 μm in diameter. Two Si(Li) X-ray detectors were used to measure the characteristic X-rays in two energy ranges: the low energy X-ray detector for 1–10 keV, and the high energy X-ray detector from 4–40 keV. The high energy X-ray detector was used for identification Tl L-lines and K-lines of Cs and I. The acceptance of the detector was 0.66 msr, and its thickness was 4.4 mm with a 12 μm thick Be window to suppress the low energy part of the spectrum. The low energy detector was used to identify possible contaminants in the scintillator material (no optically significant contaminants were found). A precision of 10 μm for positioning of the sample was provided by the stepping motor for each degree of freedom. A sketch of the setup is presented in Fig. 2.

The relative Tl concentration was measured at 10 equidistant points on both sides of the sample crystal, and at the two points of the reference crystal that were measured at LIBAF. Also, for the test sample, scans of three 5×5 mm^2 areas were performed at both ends and the center of the crystal to investigate possible local fluctuations in the Tl concentration. A typical result from the measurement is given in Fig. 3.

4. Result and discussion

4.1. Tl concentration

The characteristic K- and L-lines in the measured X-ray spectra were identified by their tabulated experimental values and the ratios of the intensities of the Tl L-peaks to the sum of Tl L-peaks and Cs and I K-peaks were used to obtain raw values for the Tl concentration. These values were calibrated using the data from the reference crystal, that was measured with the same setup, to extract absolute values. The resulting concentrations and the distribution of Tl in the sample crystal are given in Fig. 4. Calibration of these data was carried out using the point furthest from the light sensor. However, due to the negligible difference, within statistical error, between the concentrations measured in the two calibration points of the reference crystal, the choice of calibration point is of no significance for the result discussed here. The average values for the measurements on both lateral sides of the crystal were also calculated and are displayed in the same figure (black line).

Within the precision of the measurements, no clear trend in doping concentration was found neither along the main crystal axis nor between the two lateral sides. Small variations in dopant concentration were observed however. The general spread of the concentration values, that largely are within one standard deviation of each other, was reproduced by the area scans with higher statistics, which shows that a small random variation in Tl distribution over the volume of the sample cannot be excluded. It should be noted here that PIXE is a surface-oriented method and that ~90% of the Tl X-rays originate from a depth of less than 10 mg/cm^2 (~22 μm) in the current case. An average concentration was therefore extracted from the 20 measurements on the two wide lateral sides of the crystal. It was determined in this way that the concentration of Tl in the sample crystal is 0.0839(38)% by weight, where the uncertainty is calculated as the standard deviation of the Tl concentration from all the 20 measurement points. The deduced concentration is well within the range requested from the manufacturer of 0.06 – 0.12% by weight between crystals.

One should note that the measurement time was typically ca 600 s for the point measurements and ca 1200 s for the scanned areas. An improvement of the statistical error e.g. by one order of magnitude would thus require significantly longer measurement times. It can nonetheless provide further insights into detector performance if a statistical analysis based on the acquired data is conducted to determine the light output variations that can be expected from the concentration measurements. We discuss this point below.

4.2. Relating Tl concentration to light output

We point to Ref. [23] for a general discussion of Tl dopant concentration in CsI(Tl) and scintillation light output, and to the data published in Ref. [24] for the relation between relative light output and Tl concentration that we use in the following analysis. The data from Ref. [24] are given by the blue markers in Fig. 5, where a histogram showing the distribution of Tl concentration values from our measurements is given as an inset. The blue hatched region in the inset indicates the $\pm 1\sigma$ band for the Tl concentration. We have fitted the data given by the blue squares in Fig. 5, to extract an empirical relation between the relative light output, LO, and the Tl concentration using the following function:

$$\mathrm{LO} = p_0 + \frac{p_1 \exp\left[-(p_4 + p_5 C_{\mathrm{Tl}})\right]}{1 + \exp\left[-(p_2 + p_3 C_{\mathrm{Tl}})\right]}, \tag{3}$$

where C_{Tl} is the Tl concentration in % by weight and p_i are fit parameters. The result of the fit is given by the red curve in Fig. 5. The average measured Tl concentration from this work, 0.0839(38)% by weight, is given by the vertical blue line in the same figure, where the blue hatched area that surrounds it gives the statistical spread in the same way as in the inset. By applying the light-output curve to the extracted Tl concentration we conclude that the relative light output is $97.3^{+1.3}_{-1.7}$%, compared to the maximum attainable in the given range of Tl concentration according to Ref. [24]. A straightforward statistical measure of the light output non-uniformity that arises from this distribution comes from using the $\pm 1\sigma$ endpoints to calculate ΔLO. This estimate gives $\Delta\mathrm{LO} = (97.3+1.3-(97.3-1.7))/97.3 = 3.08\% \sim 3\%$ in the current case. The $\pm 2\sigma$ estimate for two independent measurement points give a light-output non-uniformity of 6% in the same manner. An alternative approach is to calculate ΔLO from the pointwise light output variation presented by the upper two curves in Fig. 4. Approximating the light output inside the crystal to be the average of the values deduced for two left and right laterally opposing points using Eq. (2) gives $\Delta\mathrm{LO} = 4.6(2.4)\%$. This value reproduces the upper bound of the source measurement discussed in Section 3 within 1.2σ. One can also use this estimate to conclude that $\Delta\mathrm{LO} \leq 4.6\%$ with 50% probability and $\Delta\mathrm{LO} \leq 4.6 - 2.4 = 2.2\%$ with only 16% probability if a normal distribution is assumed. If we suppose that the same stochastic Tl-concentration distribution can be generalized to all crystals in the right panel of Fig. 1 then the same conclusion can be drawn for the full set.

It is also clear from Fig. 5 that an increased width of the Tl distribution is mapped onto a wider range of relative light output values. Consequently, a wider Tl distribution increases, on average, the probability to find the two extreme light-output values that are used to extract ΔLO in Eq. (2) further apart. In this way a larger width of the Tl distribution results in a larger ΔLO value as e.g. plotted on the x-axis in the right panel in Fig. 1. This means that a finite width of the Tl distribution results in a minimum ΔLO value using the stochastic model discussed here.

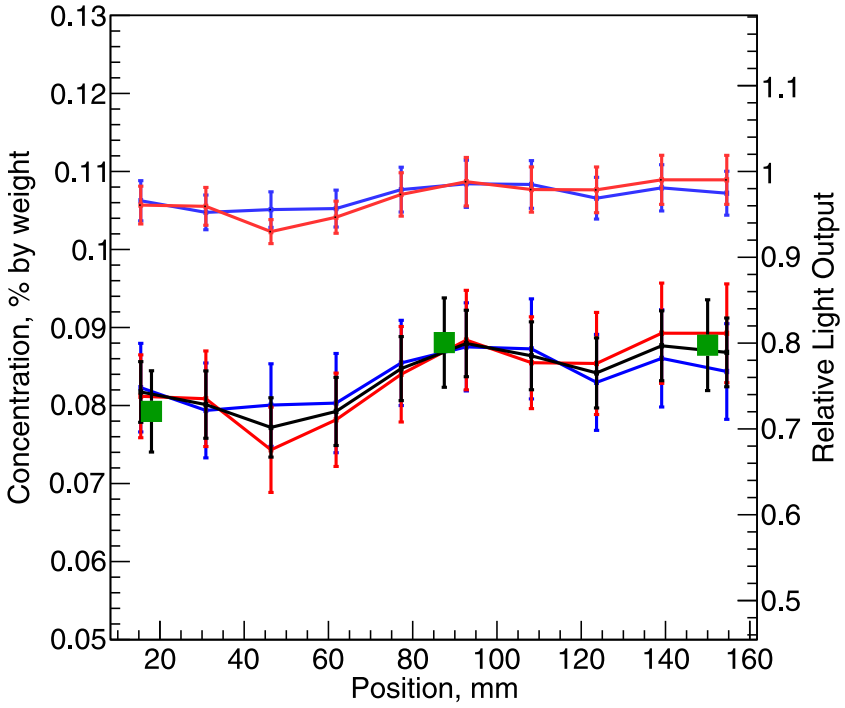

Fig. 4. The Tl concentration in per cent by weight over the length of the CsI(Tl) sample crystal. The red and blue lines show the concentration measured at the respective sides of the crystal, and the black line shows the average value (lower set of curves). The green squares indicate results of scans of 5×5 mm^2 areas. The error in concentration for the latter measurements is 0.0057% by weight. The two upper curves show the deduced variations in light output corresponding to the Tl concentrations measured for the two sides based on the data given in Fig. 5. (For interpretation of the references to color in this figure legend, the reader is referred to the web version of this article.)

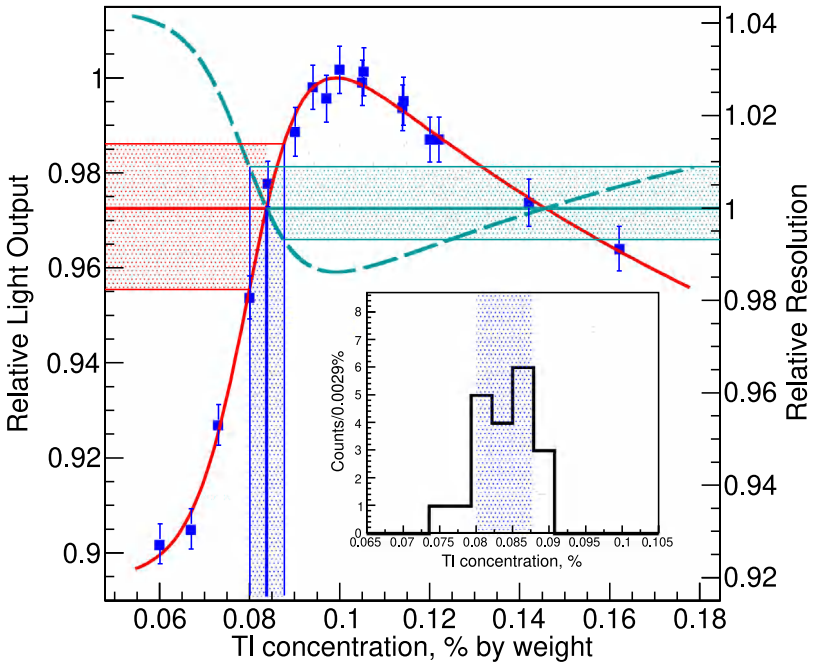

Fig. 5. The dependence of relative light output of a CsI(Tl) crystal on Tl concentration (blue markers) adapted from Ref. [24] with fitted curve (red). The vertical blue line shows the average value of the Tl concentration of 0.0839% by weight for all 20 measurement points in this study and the hatched area gives the 1σ variation of 0.0038% by weight. Taking this statistical variation in the Tl concentration into account gives a relative light output of $97.3^{+1.3}_{-1.7}$% where the statistical variation is represented by the red hatched area. The relative resolution (green dashed curve) results from applying the relation $1/\sqrt{\mathrm{LO}}$ on the light-output curve (in red). Similarly, the green hatched area provides the variation in relative resolution that corresponds to the statistical spread in the Tl concentration given above. The inset shows the distribution of the Tl concentration of the 20 measurement points and the corresponding $\pm 1\sigma$ band. (For interpretation of the references to color in this figure legend, the reader is referred to the web version of this article.)

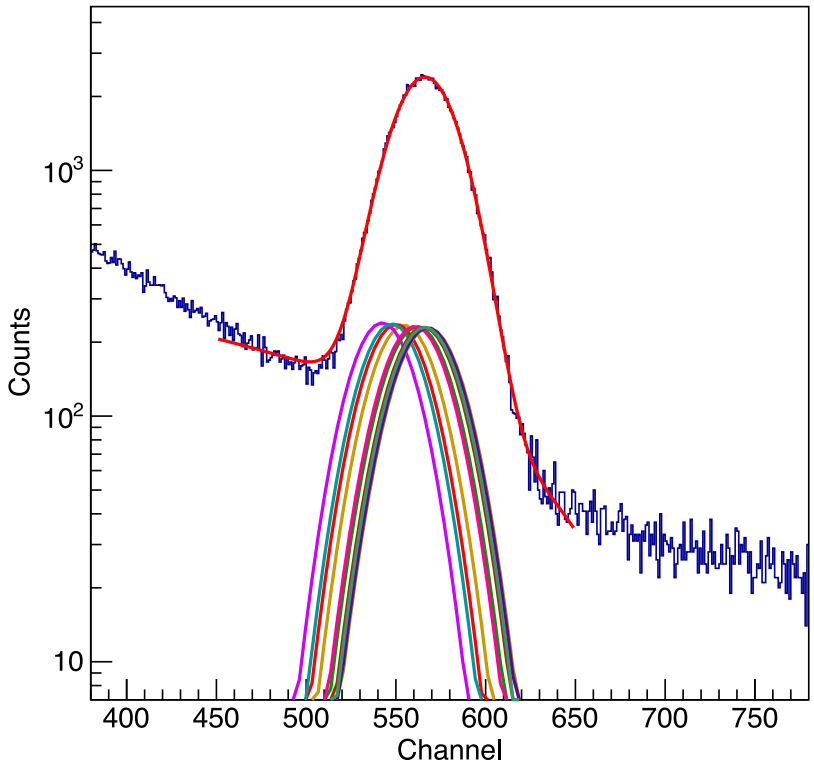

Fig. 6. The simulated sum photopeak from the Tl concentration distribution constructed from Gaussians of individual peaks. The relative light output was extracted with the formula given by Eq. (3) and scaled to the average value of the photopeak centroid calculated from the set of photopeaks obtained at 10 equidistant points measured with a collimated ^{137}Cs γ-source as shown in Fig. 1. The widths of the peaks were related to the light output assuming Poisson statistics. The resolution of the sum peak is 8.22(2)% compared to 7.74(6)% for the average of the individual peaks. For further details see the text.

4.3. Influence on the resolution

The statistical variation in the Tl concentration can also be used to estimate how the corresponding variation in light output influences the measured resolution of the sum peak mentioned in Section 3. In order to do so one should first observe that it is well established that the detection process in a scintillation detector follows Poisson statistics [21,26,27]. This means that for an event where N scintillation photons are created, and a fraction f of those is detected, then the signal amplitude will be proportional to fN, and thus to the light output LO. Consequently, the position of the centroid of the corresponding photopeak in the spectrum will be proportional to LO so that any variation in the light output, ΔLO, would move the centroid to a new position proportional to LO + δLO. Secondly, since the detection process is governed by Poisson statistics the width of the photopeak scales as $\sqrt{\text{LO}}$ and the resolution as $\sqrt{\text{LO}}/\text{LO} = 1/\sqrt{\text{LO}}$. The green curve in Fig. 5 is calculated from the fitted red curve for light output, LO, versus Tl concentration, using this relation. One can note that a Tl concentration of ~0.1% by weight should give the best resolution for a single photopeak, and that the $\pm 1\sigma$ band in Tl concentration projects on a relative resolution between 0.993 and 1.01, where we have normalized the relative resolution to one at a Tl concentration of 0.0839% per weight. A lower value of the relative resolution, given by the green curve in Fig. 5, means improved resolution and vice versa.

Based on the two observations above one can use the measured Tl concentration distribution to simulate the resolution of the sum peak discussed in Section 3. To this end a set of 10 Tl concentration values were drawn using the probability distribution given by the histogram in the inset in Fig. 5. These Tl concentrations were then propagated using the LO and $1/\sqrt{\text{LO}}$ curves in the same figure to give centroids and widths for 10 Gaussian peaks where the average width of 7.74% from the measurement in Section 3, was set to correspond to the average Tl concentration of 0.0839% per weight, i.e. to have a relative resolution of one. This means e.g. that a photopeak with a resolution of 7.74% would by scaling with $\sqrt{98.6/95.6}$ be broadened to 7.86%, for a change in the light output of 3%.

The set of peaks created in this manner (see Fig. 6) was used to generate a sum spectrum on the same background as the measurement shown in the inset of Fig. 1. Fitting a Gaussian to the sum peak gives a resolution of 8.22(2)% compared to the average resolution of the individual peaks of 7.74(6)%, thus resulting in a reduction in resolution of 0.48(6)%. This can be compared to the corresponding peak broadening observed in the measurements using side illumination with the collimated ^{137}Cs source, mentioned in Section 3 and discussed in Ref. [2], where the resolution varies from 7.74(6)% to 7.96(2)% for the summed peak, i.e. by 0.22(6)%. This value is somewhat smaller than the value extracted from the variations in Tl concentration using the method above, which can be understood from the statistics acquired in the PIXE measurements, and from the fact the PIXE measurement probes the surface of the crystal while the γ-rays also probe the internal volume. Based on this result we conclude that variations in Tl concentration in the CALIFA crystals can potentially be the cause of the lower limit in light output non-uniformity for the detector modules that can be seen in the right panel of Fig. 1, but that the effect has limited influence on the resolution.

5. Summary and conclusion

The purpose of the current study has been to quantify variations in doping concentration for a frustum-shaped sample detector, which is at the lower end of the light-output non-uniformity distribution, at a ΔLO ~ 2−3%, that we have established in earlier in measurements on a larger set of crystals (see the right panel of Fig. 1). The aim has also been to see how such variations can influence the light-output non-uniformity and resolution. The investigated sample exhibits relatively small light output variations after lapping and has a measured ΔLO =

1.59(5)%, as defined by Eq. (2), from source measurements. The result of the ΔLO measurement is presented in the left panel of Fig. 1 and the measurement procedure, using a collimated ^{137}Cs source, is described in Ref. [2].

The Tl concentration was measured along the main axis of the detector crystal using the PIXE technique, with a typical penetration depth here of ∼22 μm, in order to quantify variations in Tl concentration with position. No clear trends or gradients of the dopant concentration were observed, neither in the longitudinal nor the lateral directions. An average concentration of 0.0839(38)% by weight was measured. This value is well within the limits of the Tl concentration requested for the detector system as a whole of 0.06 – 0.12%.

The influence of the observed statistical spread in the Tl concentration on light output was deduced using an empirical relation fitted to previously published data in Ref. [24]. Based on this relation it is concluded that the observed Tl concentration corresponds to a light output of $97.3^{+1.3}_{-1.7}$%, with respect to the maximum attainable given in that study. We have taken the $\pm 1\sigma$ statistical spread in light output, ≤3%, to estimate a typical light-output non-uniformity. For the specific crystal the extracted light-output non-uniformity based on the pointwise Tl-concentration measurements is 4.6(2.4)% which reproduces the upper bound of the source measurement within 1.2σ. In addition, using a simulation approach an upper limit of the broadening of the energy resolution of 0.48(6)% was extracted for a set of 10 photopeaks whose centroids and widths were extracted from the variations in light output. This should be compared to 0.22(6)% from the corresponding measurement discussed in Section 3 and the overall resolution of 7.74%. Taken together the result suggests that variations in Tl concentration along the crystal length can potentially be the cause of the lower limit on the light output non-uniformity observed in measurements, but that this contribution to the overall resolution is comparatively small.

Finally, there is at this stage no reason to believe that this effect would be larger in other crystal samples made for CALIFA as the manufacturing procedure is the same for all the crystals. Still further work is planned concerning crystals with relatively large persistent light-output non-uniformity after lapping. The conclusions and full understanding of the performance will ultimately depend on systematic simulations of the light scintillation, transport and collection processes, for which a number of different parameters will have to be determined empirically. A variation in dopant concentration is one such parameter that has been quantified here. Others include surface properties and absorption lengths for the crystals which we addressed in Ref. [2].

CRediT authorship contribution statement

A. Knyazev: Methodology, Software, Validation, Formal analysis, Investigation, Data curation, Writing original draft, Writing - review & editing, Visualization. **J. Park:** Methodology, Software, Formal analysis, Writing - review & editing, Visualization. **P. Golubev:** Methodology, Software, Writing - review & editing. **J. Pallon:** Methodology, Validation, Formal analysis, Investigation, Writing - review & editing. **J. Cederkall:** Conceptualization, Methodology, Software, Validation, Formal analysis, Investigation, Resources, Data curation, Writing original draft, Writing - review & editing, Visualization, Supervision, Project administration. **H. Alvarez-Pol:** Conceptualization, Methodology, Software, Writing - review & editing, Supervision. **J. Benlliure:** Conceptualization, Methodology, Resources, Supervision. **J.A. Briz:** Formal analysis, Investigation. **P. Cabanelas:** Methodology, Writing - review & editing, Supervision. **E. Casarejos:** Conceptualization, Methodology. **D. Cortina-Gil:** Conceptualization, Methodology, Resources, Writing - review & editing, Supervision, Project administration. **P. Díaz Fernández:** Methodology. **M. Feijoo:** Software. **D. Galaviz:** Methodology, Validation, Supervision. **E. Galiana:** Software, Validation. **M.J.G. Borge:** Investigation, Resources, Supervision. **R. Gernhäuser:** Conceptualization, Methodology, Software, Resources, Writing - review & editing, Project administration. **D. Gonzalez:** Validation. **C. Gutierrez-Neira:** Conceptualization, Methodology, Validation, Formal analysis, Investigation. **A.-L. Hartig:** Validation, Investigation. **A. Heinz:** Methodology, Writing - review & editing, Supervision. **B. Heiss:** Software. **H. Johansson:** Methodology, Software. **P. Klenze:** Software. **T. Kröll:** Resources, Supervision, Project administration. **T. Nilsson:** Conceptualization, Methodology, Resources, Supervision, Project administration. **A. Perea:** Software, Formal analysis, Investigation. **L. Ponnath:** Software. **H.-B. Rhee:** Validation, Investigation. **J.L. Rodriguez-Sanchez:** Software. **O. Tengblad:** Conceptualization, Methodology, Resources, Writing - review & editing, Supervision, Project administration. **P. Teubig:** Methodology, Validation.

Declaration of competing interest

The authors declare that they have no known competing financial interests or personal relationships that could have appeared to influence the work reported in this paper.

Acknowledgments

Discussions with Vladimir Avdeichikov and Bo Jakobsson over several years, preceding this study, are greatly acknowledged as is the work of Robert Frost and Mikael Elfman with the preparation and setup of the beam at LIBAF, and the work of Alexandr Bobovnikov to prepare the sample crystal. This work was supported by the Swedish research council (VR) grants 2017-03986, 2014-06644, 2013-04178, 2012-04550, BMBF contracts 05P15WOFNA, 05P19WOFN1, 05P15RDFN1, 05P19RDFN1, the TU Darmstadt – GSI cooperation contract HIC for FAIR, by the Spanish National Research Council, Spain grants FPA02015-64969-P (MINDECO/FEDER/EU), FPA2015-69640-C2-1-P, PGC2018-099746-B-C21, MDM-2016.0692 (MINECO/FEDER/EU) and by GRC, Germany ED431C 2017/54 (Xunta de Galicia/FEDER/EU).

References

[1] J. Bea, et al., Simulation of light collection in scintillators with rough surfaces, Nucl. Instrum. Methods Phys. Res. A 350 (1994) 184–191.
[2] A. Knyazev, et al., Properties of the CsI(Tl) detector elements of the CALIFA detector, Nucl. Instrum. Methods. Phys. Res. A 940 (2019) 393–404.
[3] E. Auffray, et al., Crystal conditioning for high-energy physics detectors, Nucl. Instrum. Methods Phys. Res. A 486 (2002) 22–34.
[4] S. Diehl, et al., Impact of non-uniformity in light collection on the energy resolution of the PANDA electromagnetic calorimeter at photon energies below 1 GeV, J. Phys. Conf. Ser. 928 (2017) 012040.
[5] M. Durante, et al., All the fun of the FAIR: fundamental physics at the facility for antiproton and ion research, Phys. Scr. 94 (3) (2019) 033001.
[6] M. Leitner, et al., The FRIB project at MSU, in: C. Antoine, S. Bousson, G. Martinet (Eds.), Proceedings 16th International Conference on RF Superconductivity (SRF2013), JACoW, 2013, pp. 1–10.
[7] J. Dilling, R. Krücken, L. Merminga, Ariel overview, Hyperfine Interact. 225 (2014) 253–262.
[8] S. Gales, GANIL-SPIRAL2: a new era, J. Phys. Conf. Ser. 267 (2011) 012009.
[9] M.J.G. Borge, K. Blaum, Focus on exotic beams at ISOLDE: A laboratory portrait, J. Phys. G: Nucl. Part. Phys. 45 (1) (2017) 010301.
[10] G. Prete, The SPES project at the INFN-Laboratori Nazionali di Legnaro, in: Proceedings of UCANS V, 5th International Meeting of the Union for Compact Accelerator-DRiven Neutron Sources, 2015, Vol. 38 C, p. 181.
[11] H. Sakurai, RI beam factory project at RIKEN, in: INPC 2007: Proceedings of the 23rd International Nuclear Physics Conference, Vol. 805, 2008, pp. 526c–532c.
[12] D. Cortina-Gil, et al., CALIFA, a dedicated calorimeter for the R^{3}B/FAIR, Nucl. Data Sheets 120 (SI) (2014) 99–101.
[13] O. Tengblad, NUSTAR and the status of the R^{3}B project at FAIR, Pramana 75 (2010) 355–361.
[14] P. Yang, C.D. Harmon, F.P. Doty, J.A. Ohlhausen, Effect of humidity on scintillation performance in Na and Tl activated CsI crystals, IEEE Trans. Nucl. Sci. 61 (2) (2014) 1024–1031.
[15] H. Alvarez Pol, et al., Performance analysis for the CALIFA Barrel calorimeter of the R3B experiment, Nucl. Instrum. Methods. Phys. Res. A 767 (2014) 453–466.
[16] B. Pietras, M. Winkel, et al., First testing of the califa barrel demonstrator, Nucl. Instrum. Methods Phys. Res. A 814 (2016) 56–65.

[17] M. Winkel, Dissertation Dr. rer. nat, Komplexe Pulsformalgorithmen und Teilchenidentifikation zur Echtzeit-Implementierung in CALIFA, Fakultät für Physik Technischen Universität München, 2016.
[18] O. Tengblad, et al., LaBr3(Ce):LaCl3(Ce) phoswich with pulse shape analysis for high energy gamma-ray and proton identification, Nucl. Instrum. Methods Phys. Res. A 704 (2013) 19–26.
[19] G.F. Knoll, Radiation detection and measurement, fourth ed., Wiley, New York, NY, 2010, p. 830.
[20] M. Moszynski, Energy resolution of scintillation detectors, in: R.B. James, L.A. Franks, A. Burger (Eds.), Hard X-Ray and Gamma-Ray Detector Physics VII, Vol. 5922, International Society for Optics and Photonics, SPIE, 2005, pp. 16–29.
[21] J.B. Birks, The Theory and Practice of Scintillation Counting, Pergamon Press, 1964, pp. 97–99.
[22] L. Trefilova, et al., Photo- and radiation-stimulated processes in CsI(Tl) crystals, IEEE Trans. Nucl. Sci. 55 (3) (2008) 1263–1269.
[23] L. Trefilova, et al., Concentration dependence of the light yield and energy resolution of NaI:Tl and CsI:Tl crystals excited by gamma, soft x-rays and alpha particles, Nucl. Instrum. Methods Phys. Res. A 486 (2002) 474–481.
[24] A. Gektin, et al., Light output tuning for the long-length CsI(Tl) scintillators, Nucl. Instrum. Methods Phys. Res. A 598 (2009) 270–272.
[25] N. Grassi, et al., Pixe characterization of CsI(Tl) scintillators used for particle detection in nuclear reactions, Nucl. Instrum. Methods Phys. Res. B 266 (2008) 2383–2386.
[26] W.R. Leo, Techniques for nuclear and particle physics experiments, Springer-Verlag, 1994, p. 117.
[27] K.S. Krane, Introductory Nuclear Physics, John Wiley and Sons, 1988, p. 224.